

## A rational approach to form disulfide-linked mucin hydrogels

Katherine Joyner<sup>1\*</sup>, Daniel Song<sup>1\*</sup>, Robert F. Hawkins<sup>1</sup>, Richard D. Silcott<sup>1</sup>, Gregg A. Duncan<sup>1,2</sup>

<sup>1</sup>Fischell Department of Bioengineering, University of Maryland, College Park, MD 20742

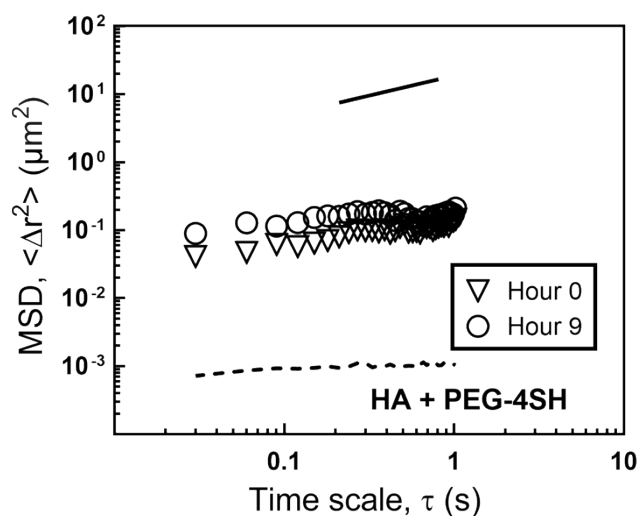
<sup>2</sup>Biophysics Program, University of Maryland, College Park, MD 20742

\*These authors contributed equally to this work

Correspondence to: Gregg Duncan; email: [gaduncan@umd.edu](mailto:gaduncan@umd.edu)

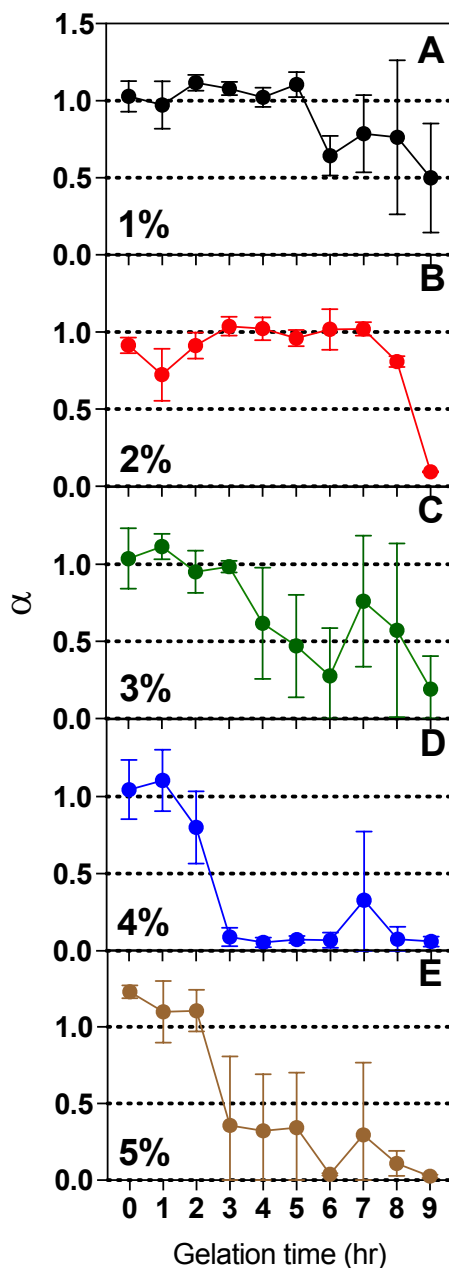
### Supporting Information

Figure S1



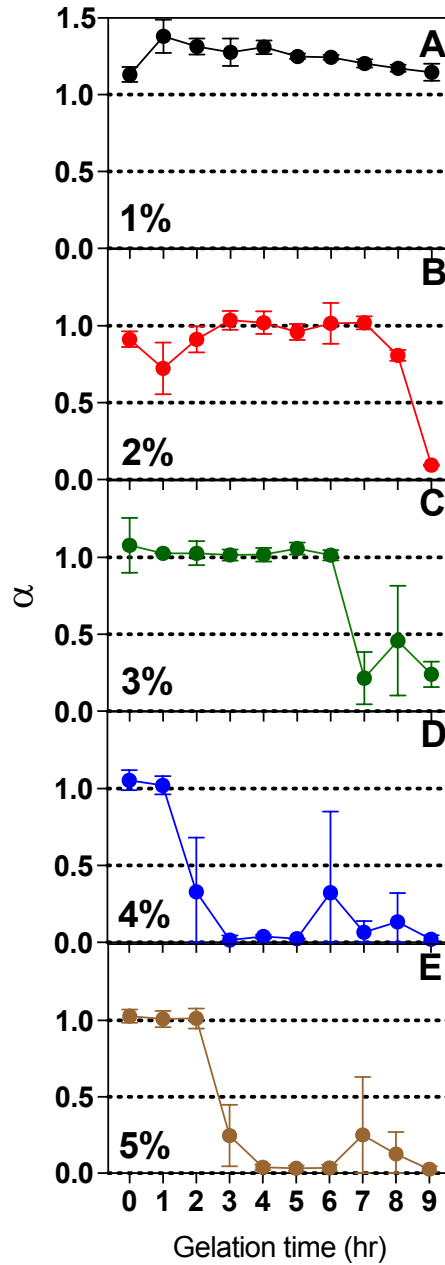
**Figure S1. Microrheology of PEG-4SH mixed with hyaluronic acid.** Multiple particle tracking of 100 nm PEG-NP in 2% w/v PEG-4SH mixed with 2% hyaluronic acid 500 kDa (Lifecore Biomedical). The ensemble average mean squared displacement as function of time scale  $\tau$  (MSD;  $\langle \Delta r^2 \rangle$ ) of 100 nm PEG-NP at hour 0 (triangles) and hour 9 (circles). Solid line with slope  $n=0.5$  and dashed line of 2% PGM/PEG-4SH hydrogel are also shown for reference.

Figure S2



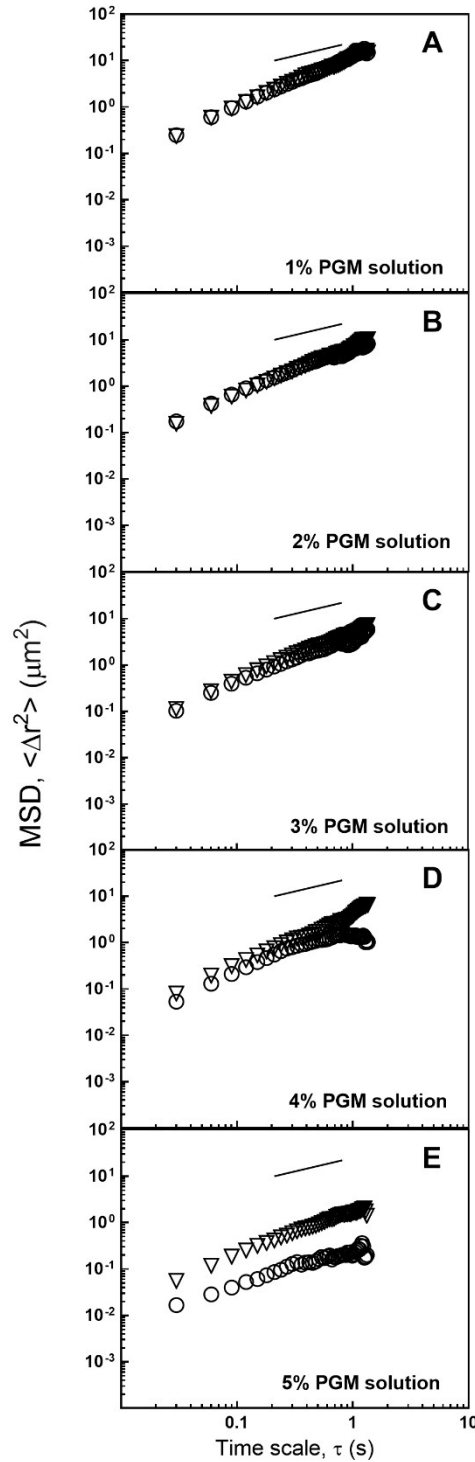
**Figure S2. Gelation rate of mucin-based hydrogels with varying PGM concentration with a constant PEG-4SH concentration of 2% w/v.** Individual experiments using increasing PGM concentrations in w/v of (A) 1% (black), (B) 2% (red), (C) 3% (green), (D) 4% (blue), and (E) 5% (brown) are shown. Kinetics of PGM gel formation as analyzed by microrheology using 100 nm PEG-NP probes. The gelation point is measured as  $\alpha = 0.5$ . Each panel displays the mean and standard error of measured  $\alpha$ .

Figure S3



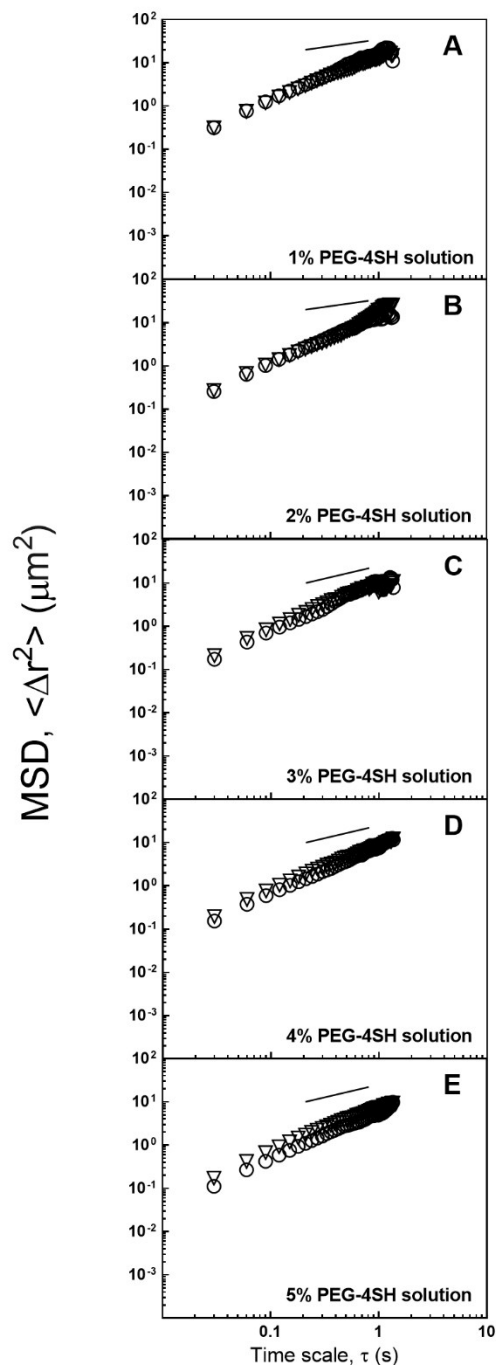
**Figure S3. Gelation rate of mucin-based hydrogels with varying PGM concentration with a constant PEG-4SH concentration of 2% w/v.** Individual experiments using increasing PEG-4SH concentrations in w/v of (A) 1% (black), (B) 2% (red), (C) 3% (green), (D) 4% (blue), and (E) 5% (brown) are shown. Kinetics of PGM gel formation as analyzed by microrheology using 100 nm PEG-NP probes. The gelation point is measured as  $\alpha=0.5$ . Each panel displays the mean and standard error of measured  $\alpha$ .

Figure S4



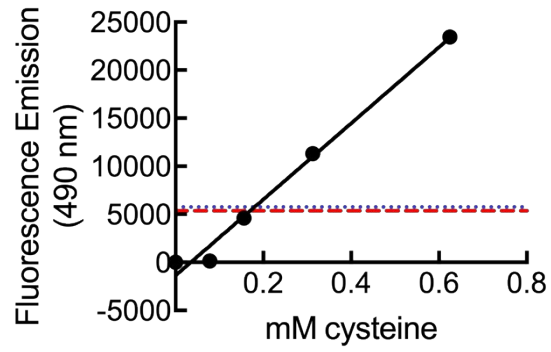
**Figure S4. Microrheology of PGM solutions.** Multiple particle tracking of 100-nm PEG-NP in individual solutions of PGM with concentrations in w/v of (A) 1%, (B) 2%, (C) 3%, (D) 4%, and (E) 5% are shown. The ensemble average mean squared displacement as function of time scale  $\tau$  (MSD;  $\langle \Delta r^2 \rangle$ ) of 100 nm PEG-NP at hour 0 (triangles) and hour 9 (circles). A reference line with slope  $n=0.5$  is included.

Figure S5



**Figure S5. Microrheology of 4-arm PEG-thiol solutions.** Multiple particle tracking of 100-nm PEG-NP in individual solutions of 4-arm PEG-thiol with concentrations in w/v of (A) 1%, (B) 2%, (C) 3%, (D) 4%, and (E) 5% are shown. The ensemble average mean squared displacement as function of time scale  $\tau$  ( $MSD; \langle \Delta r^2 \rangle$ ) of 100 nm PEG-NP at hour 0 (triangles) and hour 9 (circles). A reference line with slope  $n=0.5$  is included.

**Figure S6**



**Figure S6. Total cysteine content of PGM and BSM solutions.** Total cysteine concentration of each mucin solution based on linear regression analysis of L-cysteine standards (black;  $r^2=0.98$ ). The fluorescence was measured at excitation and emission wavelengths of 395 and 490 nm, respectively. Measurements for each mucin are shown as lines for BSM (dotted blue) and PGM (dashed red).